High resolution simulations dramatically improve predictions of low-frequency Pacific basin sea level variability

Christopher Little (clittle@aer.com) (AER, Inc); Stephen Yeager and John Fasullo (NCAR), Steve Nerem and Kris Karnauskas (UC Boulder)

Motivation and Background

The bad: Coarse resolution model simulations fail to reproduce observed trends in the Pacific basin in, e.g., surface air temperature and sea level pressure (e.g., Wills et al. 2022).

The good: High resolution initialized predictions better represent low-frequency variability, particularly in the tropical Pacific and Southern Oceans (Yeager et al. 2022; Y22).

Our question: Do the resolution-related improvements found in Y22 extend to [coastal] sea level?

To address this question, we use altimetric observations to assess lead year 1-5 predictions of linear trends in dynamic sea level from initialized low-resolution (DPLE) and high-resolution (HRDP) decadal prediction simulations, conducted with the Community Earth System Model. Because basin-wide altimetry is only available after 1993, we develop a longer verification dataset using >30 tide gauge records.

Altimeter-era dynamic sea level trends

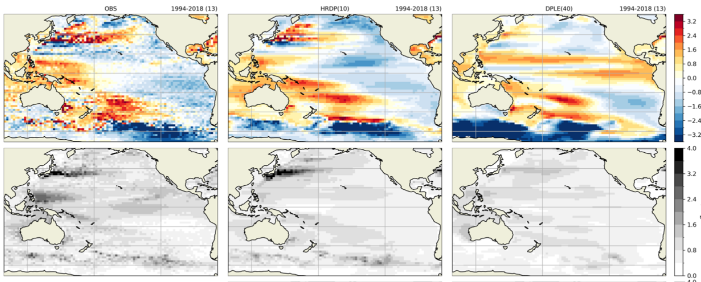

$$\zeta(x,y,t,m) = [\alpha(x,y,m) \pm \sigma](t-t_0) + \beta$$

$$\sigma_{trend}(x,y) = \frac{1}{n}\sum_{n=1}^{10} \sigma(x,y,m)$$

$$\alpha(x,y) = \bar{\alpha}(x,y) \pm \sigma_{ens}$$

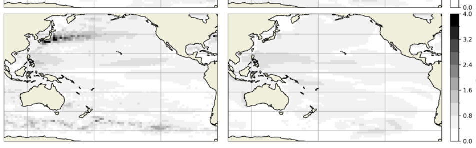

(Top row) Linear dynamic sea level trends from altimetry (MEASURES 1/6º; Fournier et al. 2022; left), HRDP (middle), and DPLE (right) over the time windows indicated, after regridding to a common 2º grid. All datasets have been sampled to match the every-other-year temporal sampling of HRDP. The number in parentheses indicates the sample size used for trend computation. Trends are calculated for predictions (mean of 10 ensemble members, averaged over forecast years 1-3) for HRDP and DPLE, and 3-year rolling mean for altimetry. (Middle row) Error in linear trend (mean of 10 ensemble members for HRDP and DPLE). (Bottom row) Ensemble standard deviation in linear trend estimate.

Consistency of linear trends (1993-2019)

HRDP - Altimetry $\Delta = \bar{\alpha}_{model}(x,y) - \alpha_{obs}(x,y)$ **DPLE - Altimetry**

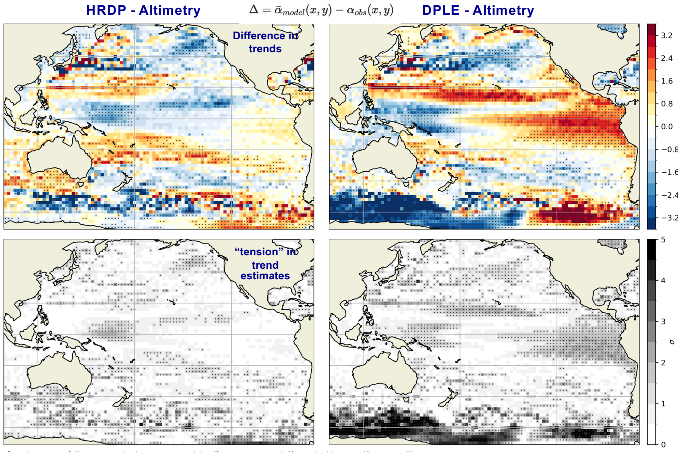

Consistency of linear trends between models (forecast year 1-3) and altimetry (3-year rolling mean). (Top row) Shading represents the differences in ensemble-mean linear sea level trends and altimetry for HRDP (left) and DPLE (right). (Bottom row) Model-data consistency in linear trends, expressed as “tension” (T) between linear trend estimates. Stippling indicates T>1.

$$T = \frac{\Delta}{\sigma_{tot}} \quad \sigma_{tot} = \sqrt{{\sigma_e}^2 + \sigma_{t,model}^2 + \sigma_{t,obs}^2}$$

Sensitivity to forecast lead year

Altimetry **HRDP - Altimetry** **DPLE - Altimetry**

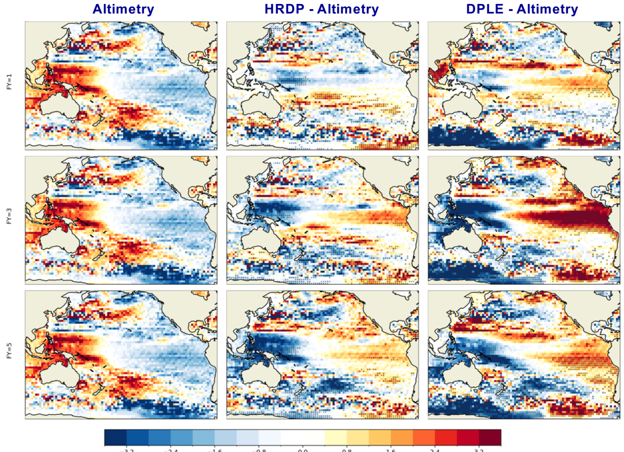

Sensitivity of predictions to forecast lead year. Linear trends from altimetry (left), and the differences between altimetry and HRDP (middle; mean of ensemble members), and DPLE (right; mean of ensemble members) over the time windows indicated, as a function of forecast year. All datasets have been sampled to match the every-other-year temporal sampling of HRDP. The number in parentheses indicates the sample size used for trend computation. Stippling indicates T>1.

Conclusions

- ☆ Predictions of low-frequency dynamic sea level variability are greatly improved in HRDP relative to the DPLE in the tropical Pacific, Southeast Pacific, and Southern Oceans
- ☆ Improvements are evident over long (>5 year) forecast lead times in the eastern Pacific, consistent with analyses of surface temperature and sea level pressure (See Y22, and Ping Chang's presentation Friday for potential mechanisms underlying improvements).
- ☆ HRDP improvements persist over the pre-altimeter era, at basin- and local-scales, although the period of comparison is short and observed trends are weaker
- ☆ Tide gauge records suggest that the altimeter-era zonal dynamic sea level dipole was preceded by a multidecadal sea level trend of opposite sign

Extending the comparison using the tide gauge record

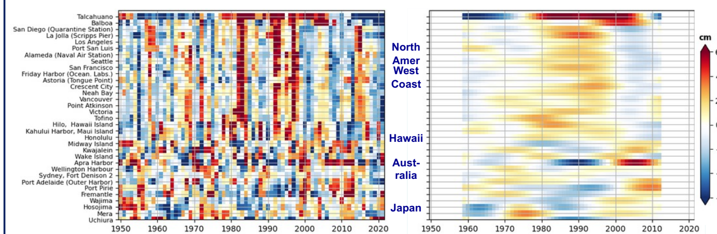

(Left) 1950-2021 detrended tide gauge sea level after removal of the inverse barometer effect (using ERA5) and global mean sea level change (using MEASURES GMSL product). A criterion of no years with missing data provides a reasonable distribution of tide gauges across the basin. While 1950-2021 trends are explicitly removed, nonlinearities and apparent trends over shorter intervals are not. (Right) 19-year low pass filtered sea level anomaly. Note non-linear behavior that differs in sign west and east, with a declining trend evident after 1990 that is strongest on the eastern margin of the basin.

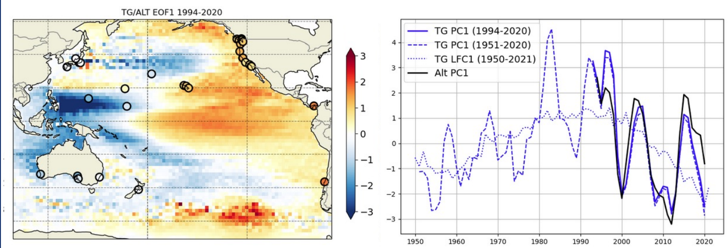

Principal component analysis indicates a basin scale mode in the tide gauge record. (Left) EOF1 from altimetry and tide gauges (3-year rolling mean) over the 1993-2021 period. (Right) PC1 from various EOF analyses for altimetry, and from tide gauges, using different time periods and techniques, including low-frequency component analysis (Wills et al., 2020). EOF1 patterns from tide gauges are very similar across time periods and techniques.

Basin-scale variability

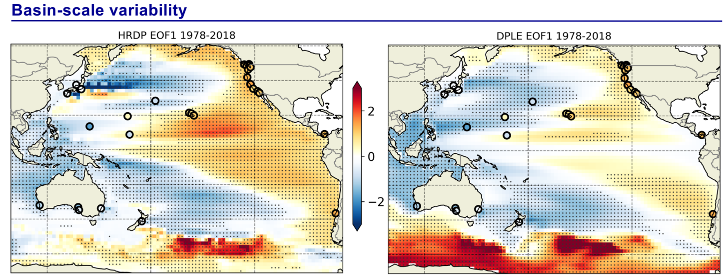

Comparison of leading EOFs from tide gauges and model simulations. (Top row) ensemble-mean EOF1 pattern for HRDP over the 1978-2018 period. Stippling is shown where the absolute value of the ensemble mean is greater than twice the ensemble standard deviation. The tide gauge EOF1, sampled at the same times as HRDP, is overlaid at tide gauge locations. (Middle row) Same as left, for DPLE. (Right) corresponding PC1 time series for each ensemble member (dotted lines) and the ensemble mean PC1 (thick lines). Ensemble mean trends are weaker in both HRDP and DPLE before 1993, consistent with tide gauges. However, the EOF is dominated by the trend, so it is difficult to see a clear improvement in the 1976-1993 period.

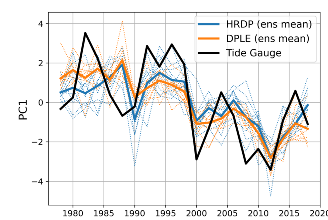

Local variability

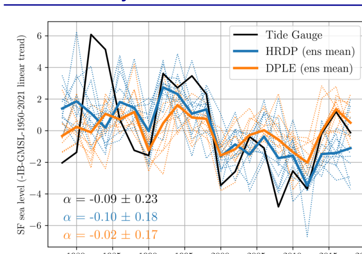

Comparison of “corrected” sea level from the San Francisco tide gauge (black line), and HRDP (blue lines) and DPLE (orange lines) predictions (FY 1-3 mean) at the closest grid point. Individual ensemble members (10) are shown with dotted lines; the ensemble mean is shown with a thick line. While it is worth exercising caution in this direct comparison, due to the different processes driving sea level at tide gauges and in the DP simulations, linear trends (shown in plot) are much more consistent in HRDP than DPLE. Both ensemble mean projections indicate a strengthening of the downward trend over time.

Fournier S., Willis J., Killett E., Qu Z. and Zlotnicki V.. 2022. JPL MEaSUREs Gridded Sea Surface Height Anomalies Version 2205. Ver. 2205. PO.DAAC, CA, USA.

Wills, R. C. J., Dong, Y., Proistosecu, C., Armour, K. C., & Battisti, D. S. (2022). Systematic climate model biases in the large-scale patterns of recent sea-surface temperature and sea-level pressure change. Geophysical Research Letters, 49, e2022GL100011. https://doi.org/10.1029/2022GL100011

Wills, R.C., T. Schneider, J.M. Wallace, D.S. Battisti, and D.L. Hartmann, 2018: Disentangling global warming, multidecadal variability, and El Niño in Pacific temperatures. Geophysical Research Letters, 45, doi:10.1002/2017GL076327.

Yeager, S.G., Chang, P., Danabasoglu, G. et al. Reduced Southern Ocean warming enhances global skill and signal-to-noise in an eddy-resolving decadal prediction system. npj Clim Atmos Sci 6, 107 (2023). https://doi.org/10.1038/s41612-023-00434-y

Thanks to the Permanent Service for Mean Sea Level (http://www.psmsl.org/data/obtaining/), for tide gauge data; NCAR for model output and processing/analysis platforms; NSF-OCE-2148507: A global assessment of annual to decadal sea level predictability, and the CIRES visiting fellows program, for support.